Heliyon 10 (2024) e35728

Contents lists available at ScienceDirect

Heliyon

journal homepage: www.cell.com/heliyon

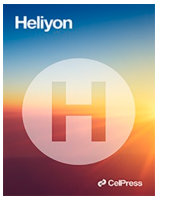

Research article

Mechanism of Chaihuang-Yishen formula to attenuate renal fibrosis in the treatment of chronic kidney disease: Insights from network pharmacology and experimental validation

Jie Miao [a,1], Cong Wei [b,1], Hong-Lian Wang [c,d], Yu-Qing Li [a], Xin-Ming Yu [a], Xiu Yang [a], Hong-Wei Su [e], Ping Li [f,**], Li Wang [c,*]

[a] College of Integrated Chinese and Western Medicine, The Affiliated Traditional Chinese Medicine Hospital, Southwest Medical University, Luzhou, China
[b] The Clinical Laboratory of the Affiliated Traditional Chinese Medicine Hospital, Southwest Medical University, Luzhou, China
[c] Research Center for Integrative Medicine, The Affiliated Traditional Chinese Medicine Hospital, Southwest Medical University, Luzhou, China
[d] Chengdu University of Traditional Chinese Medicine, Chengdu, China
[e] The Department of Urology, The Affiliated Traditional Chinese Medicine Hospital, Southwest Medical University, Luzhou, China
[f] Beijing Key Laboratory for Immune-Mediated Inflammatory Diseases, Institute of Clinical Medical Sciences, China-Japan Friendship Hospital, Beijing, China

A R T I C L E I N F O

Keywords:
Chaihuang-Yishen formula
Renal fibrosis
Chronic kidney disease
SRC
AKT1
Network pharmacology

A B S T R A C T

Renal fibrosis represents a pivotal characteristic of chronic kidney disease (CKD), for which effective interventions are currently lacking. The Src kinase activates the phosphatidylinositol-3 kinases (PI3K)/Akt1 pathway to promote renal fibrosis, casting a promising target for anti-fibrosis treatment. Chaihuang-Yishen formula (CHYS), a traditional Chinese medicinal prescription, has a validated efficacy in the treatment of CKD, however, with the underlying mechanism unresolved. This study aimed to uncover the pharmacological mechanisms mediating the effect of CHYS in treating renal fibrosis using network pharmacology followed by experimental validation. The chemical compounds of CHYS were retrieved from the Traditional Chinese Medicine Systems Pharmacology (TCMSP) database or published literature, followed by the prediction of their targets using SwissTargetPrediction software. Disease (CKD/renal fibrosis)-related targets were retrieved from the Genecards database. Protein-protein interaction (PPI) network was generated using the drug-disease common targets and visualized in Cytoscape software. The drug-disease targets were further subjected to Gene Ontology (GO) and Kyoto Encyclopedia of Genes and Genomes (KEGG) enrichment analyses by Metascape software. Additionally, the compound-target-pathway network was established in Cytosape to identify key compounds, targets, and pathways. Network pharmacology analysis screened out 96 active compounds and 837 potential targets within the 7 herbal/animal medicines of CHYS, among which 237 drug-disease common targets were identified. GO and KEGG analysis revealed the enrichment of fibrosis-related biological processes and pathways among the 237 common targets. Compound-target-pathway network analysis highlighted protein kinases Src and Akt1 as the top two targets associated with the anti-renal fibrosis effects of CHYS. In UUO mice, treatment with CHYS attenuates renal

* Corresponding author.
** Corresponding author.
E-mail addresses: lp8675@163.com (P. Li), wangli120@swmu.edu.cn (L. Wang).
[1] These authors contributed equally to this work and share first authorship.

https://doi.org/10.1016/j.heliyon.2024.e35728
Received 10 April 2024; Received in revised form 31 July 2024; Accepted 2 August 2024
Available online 8 August 2024

fibrosis, accompanied by suppressed expression and phosphorylation activation of Src. Unlike Src, CHYS reduced Akt1 phosphorylation without affecting its expression. In summary, network pharmacology and in vivo evidence suggest that CHYS exerts its anti-renal fibrosis effects, at least in part, by inhibiting the Src/Akt1 signaling axis.

Abbreviations

AKI	acute kidney injury
CH	Chaihu
CHYS	Chaihuang-Yishen formula
CKD	chronic kidney disease
CSL	Chuanshanlong
DG	Danggui
DL	druglikeness
DN	diabetic nephropathy
ECM	extracellular matrix
GFR	glomerular filtration rate
HQ	Huangqi
IRB	irbesartan
MMT	macrophage to myofibroblast transition
OB	oral availability
PPI	Protein-protein interaction
SZ	Shuizhi
SW	Shiwei
TCM	Traditional Chinese Medicine
TCMSP	Traditional Chinese Medicine Systems Pharmacology Database and Analysis Platform
UUO	unilateral ureter obstruction
ZL	Zhuling.

1. Introduction

Chronic kidney disease (CKD) is a global health issue with a higher prevalence in high and middle-income countries. CKD is staged based on the degree of glomerular filtration rate (GFR) decline [1]. Regardless of the underlying cause, all forms of CKD exhibit a common pathological hallmark known as renal fibrosis. Renal fibrosis is characterized by the expansion of the interstitial space, excessive accumulation of extracellular matrix, and progressive loss of renal parenchyma [2]. The degree of renal fibrosis is closely correlated with the decline in renal function observed in CKD [3]. Consequently, strategies aimed at mitigating renal fibrosis are considered pivotal in the management of CKD, although such approaches are currently underdeveloped. Given that the majority of CKD cases are asymptomatic and fibrotic changes are irreversible once established [1], there is an urgent need to identify pharmaceutical agents capable of combating renal fibrosis.

Table 1
Constituents of CHYS.

Name of individual herbal medicine in Latin	Chinese name	ID	Compatibility of TCM	Function exerted in the prescription	Mass ratio (%)
Astragalus membranaceus (Fisch.) Bunge	Huangqi	HQ	Monarch drug	Strengthening *qi*, dispelling pathogenic wind, and warming *yang* to promote blood circulation.	23.5
Discorea nipponica Makino	Cancanning	CSL	Minister drug	Promoting blood circulation, clearing up blood circulation, dispelling wind, and removing dampness.	17.6
Bupleurum chinense DC.	Chaihu	CH	Minister drug	Dispersing and reducing fever, relieving liver and depression, raising *yang* energy.	11.8
Angelica sinensis (Oliv.) Diels	Danggui	DG	Minister drug	Promoting blood circulation, tonifying blood, regulating menstruation, relieving pain, and promoting secretion of body fluids to move bowels.	11.8
Pyrrosia lingua (Thunb.) Farw	Shiwei	SW	Assistant drug	Inducing diuresis, promoting bowel movements, clearing heat, and stopping bleeding.	14.1
Polyporus umbellatus (Pers.) Fries	Zhuling	ZL	Assistant drug	Inducing diuresis and removing dampness.	14.1
Whitmania pigra Whitman	Shuizhi	SZ	Courier drug	Promoting blood circulation and resolving stasis.	7.1

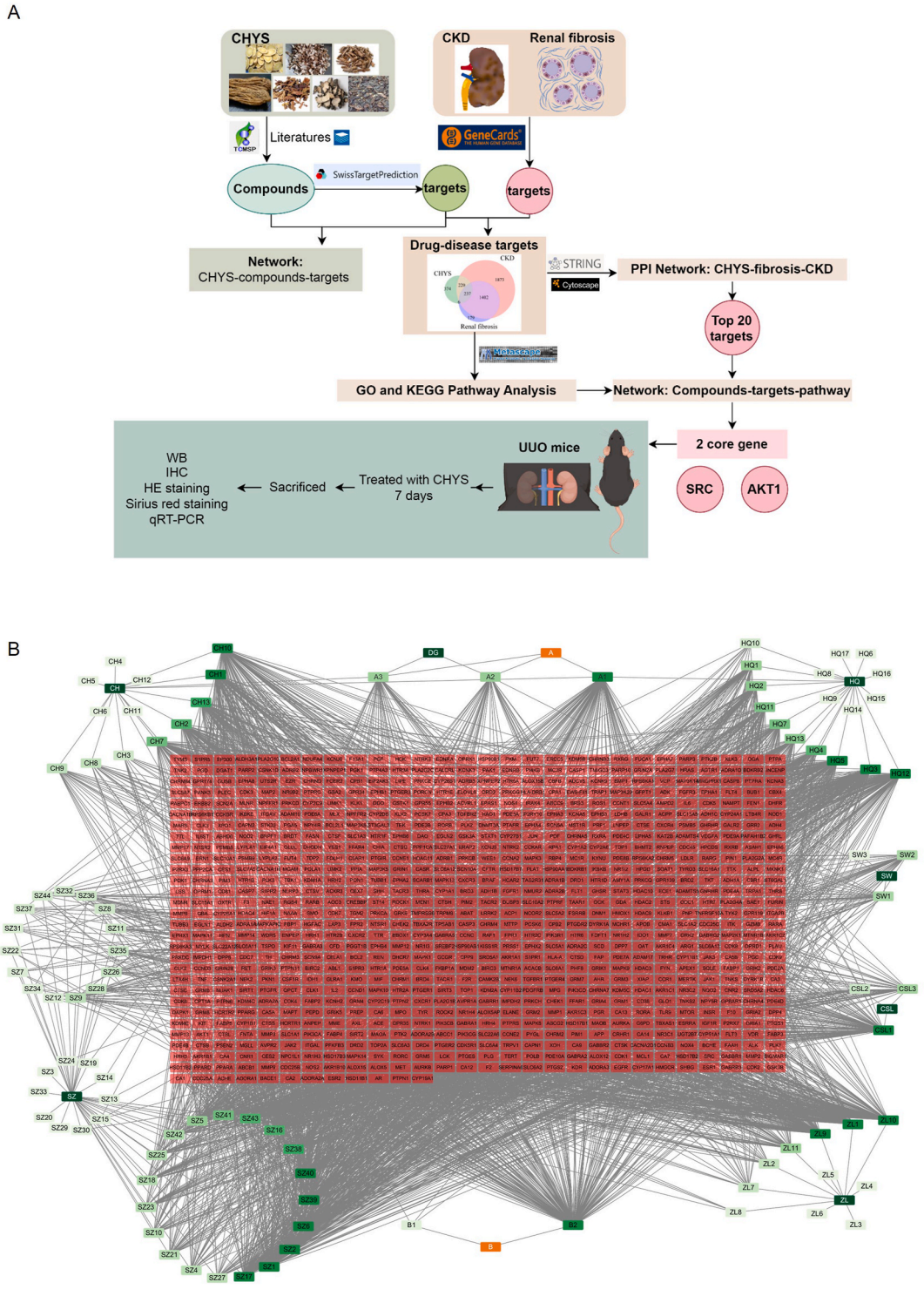

Fig. 1. Study design and CHYS-compound-target network analysis. (A) The flowchart illustrates the comprehensive methodology encompassing network pharmacology and animal experiment undertaken in this study. (B) The CHYS-compound-target network. Active compounds are depicted as green rectangles, wherein the intensity of color corresponds to the number of gene targets linked to each active compound. The associated herbal/animal medicines are positioned centrally within the compounds. Gene targets are represented by red rectangles. Notably, duplicate and triplicate compounds among HQ, CH, DG, and SW are delineated separately (orange rectangles) to ensure clarity and avoid redundancy within the network visualization.

Traditional Chinese medicine (TCM) is a popular treatment option extensively utilized in oriental countries for various forms of CKD [4]. TCM formulations typically consist of a blend of different herbal, animal, and mineral ingredients, resulting in a complex mixture containing multiple bioactive compounds that presumably target various pathological pathways involved in the disease process [4]. According to TCM principles, CKD is believed to stem from deficiencies in *qi* and blood, compounded by TCM symptoms such as blood stasis, phlegm dampness, and toxic heat, which collectively disrupt the body's *yin-yang* balance [4]. Therefore, the primary objective of TCM therapy is to replenish qi, enhance blood circulation, and eliminate dampness.

A large-scale retrospective cohort study has demonstrated the long-term benefits of combining TCM with conventional Western medical approaches in improving the survival rates of CKD patients [5]. Additionally, the efficacy of TCM in treating specific types of CKD has been supported by rigorously designed clinical trials. For instance, the TCM Tangshen formula confers additional benefits when used alongside conventional therapies in reducing proteinuria and enhancing GFR in patients with diabetic nephropathy (DN), as evidenced by a multicenter, double-blinded, randomized, placebo-controlled trial [6].

The Chaihuang-Yishen formula (CHYS), previously known as the Qilong-Lishui formula, is a patented TCM prescription widely used in clinical practice for the treatment of DN [7]. CHYS consists of six herbal medicines and one animal medicine whose detailed constituents are outlined in Table 1. Presumably, CHYS exerts its therapeutic effects by tonifying *qi*, promoting blood circulation, and facilitating diuresis. Laboratory investigations have demonstrated that CHYS can reduce proteinuria and ameliorate glomerular injury and tubulointerstitial fibrosis in DN rats induced by streptozocin [7]. Furthermore, CHYS exhibits a protective effect against renal injury in animal models of CKD induced by 5/6 nephrectomy, puromycin aminonucleoside, and unilateral ureter obstruction (UUO) [8–11].

Despite the advancements mentioned, the specific active compounds and molecular mechanisms responsible for the renoprotective effects of CHYS in CKD are still not well understood. This study aimed to elucidate the active compounds and their corresponding targets and pathways that mediate the anti-renal fibrosis effects of CHYS using a combination of network pharmacology analysis and experimental validation. The overall study design is outlined in Fig. 1A.

2. Materials and methods

2.1. Screen of active compounds and potential targets of CHYS

The active compounds in the six herbal medicines of CHYS were obtained from the Traditional Chinese Medicine Systems Pharmacology Database and Analysis Platform (TCMSP, https://www.tcmspw.com/tcmsp.php). These compounds were then filtered based on criteria including oral availability (OB) $\geq$ 30 % and drug likeness (DL) $\geq$ 0.18. Due to the absence of leech (*Whitmania pigra* Whitman, Shuizhi in Chinese) in the TCMSP database, the active compounds of leech were gathered from published literature and subjected to filtration using the web-based SwissADME software (http://www.swissadme.ch/). The filtration criteria included high gastrointestinal absorption and compliance with at least two of the five drug likeness parameters (Lipinski, Ghose, Veber, Egan, and Muegge). Subsequently, all identified active compounds underwent target prediction using the web-based SwissTargetPrediction software (http://www.swisstargetprediction.ch/). The target filtration criteria included specifying the species as *Homo sapiens* and setting a minimum possibility score of $\geq$0.6.

2.2. Screen of disease targets

Disease target genes were screened using the GeneCards database by searching with keywords "renal fibrosis" or "chronic kidney disease" with species restricted to "*Homo sapiens*". After deduplication, only target genes with a "relevance score" exceeding 10 were selected for subsequent analysis.

2.3. Construction of protein-protein interaction (PPI) network

The protein-protein interaction (PPI) network was constructed using the STRING database (https://string-db.org/) using the shared target genes between the disease (CKD/Renal fibrosis) and the drug (CHYS). The analysis was conducted with the species parameter set to "*Homo sapiens*" and the analysis mode set to "multiple proteins." The resulting network was visualized using Cytoscape 3.10 software. To identify hub genes within the network, the degree of centrality of each node (target gene) was calculated using the Cytoscape software. The top 20-ranked targets with the highest degree of centrality were selected for a second round of PPI network construction and visualization using Cytoscape software.

2.4. GO and KEGG

The drug-disease common target genes were imported into Metascape (https://www.metascape.org) for Gene Ontology (GO) and Kyoto Encyclopedia of Genes and Genomes (KEGG) enrichment analysis, using the default parameters.

2.5. Compound-target-pathway network analysis

Compound-target-pathway network was constructed using the CHYS-derived active compounds, top-ranked targets, and pathways by Cytoscape software. Using the network analyzer in Cytoscape software, topological parameters were calculated and ranked, and the

importance of the top 20 genes in this network was visualized in descending order of significance.

2.6. Animal experiment

For the animal experiment, CHYS in the form of herbal medicine granules were purchased from the Kangrentang Pharmacy Co. Ltd. The herbal medicine granules were freshly blended in warm water prior to administration to the animals. The recommended administration dose of CHYS in human is 25.3 g/60 kg, with an equivalent dose of 3.8 g/kg in mice after dose conversion based on body surface area difference. Therefore, the mice were treated with 3.8 (low dose) and 7.6 g/kg (high dose) CHYS, respectively, in the animal study.

Male C57BL/6 mice aged 8–12 weeks were purchased from Gempharmatech Co, Ltd. and housed in a specific-pathogen-free facility under a 12 h light/dark cycle with *ad libitum* access to water and rodent chow. After acclimatization for one week, the mice were randomly assigned to Sham, UUO, CHYS-L, CHYS–H, and irbesartan (IRB) groups, with each group comprising 6 mice. UUO and Sham surgeries were performed as previously described [12]. Following surgery, UUO mice in the CHYS-L and CHYS–H groups received 3.8 and 7.6 g/kg/day CHYS (dissolved in water), respectively, by gavage for 7 days. UUO mice in the IRB group were administrated with 20 mg/kg/day irbesartan by gavage for the same period. Simultaneously, mice in the Sham and UUO groups were treated with an equivalent volume of solvent. At the end of the experiment, the mice were anesthetized with pentobarbital sodium (1.5 mg/kg) followed by cervical dislocation. The kidneys from the site of UUO or Sham surgery were harvested. Half of each kidney was fixed for histological analysis, while the cortex of the remaining half was snap-frozen in liquid nitrogen and stored at −80 °C for RNA and protein analysis. All animal procedures were conducted in accordance with the regulations established by the Animal Ethics Committee of Southwest Medical University (Ref. No. 20221205-031).

2.7. Histology

The paraffin-embedded kidneys were sliced into 4 μm thick sections. After dewaxing in xylene and rehydration in a series of ethanol solutions, sections were subjected to hematoxylin and eosin (HE) staining, Sirius red staining, and Periodic Acid-Schiff (PAS) according to established protocols [13,14]. The tubular injury score was calculated as the number of tubules showing necrosis, degeneration, dilation, or intratubular cast per view field. Images were captured with an upright light microscope (Leica, ICC50W, Germany).

2.8. Immunohistochemistry

For immunohistochemistry (IHC), rehydrated kidney sections were processed using a previously described protocol [12]. Images were captured as described above. The positive staining area was quantified using ImageJ 1.47v software (NIH, USA). Details of the antibodies used in this study are provided in Supplementary Table 1.

2.9. RT-PCR

Total RNA was extracted from kidney tissues using the Trizol reagent. Subsequently, 1 μg of RNA was reverse transcribed, and the resulting cDNA was subjected to RT-PCR amplification according to established protocols [12]. Gene expression levels were normalized to the housekeeping gene GAPDH using the 2ˆ-ΔΔCt method. Primer sequences used in the RT-PCR assay are provided in Supplementary Table 2.

2.10. Western blot

Proteins from kidney tissues were extracted using RIPA buffer. The protein concentration was determined using the Ori Instant BCA Protein Quantification Kit (Oriscience, Cat# PD101, China). Subsequently, 15 μg of protein was subjected to Western blot analysis according to established protocols [12]. The intensity of protein bands was quantified using ImageJ 1.47v software (NIH, USA). The expression levels of the target proteins were normalized to GAPDH. Details of the antibodies used in the Western blot assay are provided in Supplementary Table 1.

2.11. Statistics

Quantitative data are presented as mean ± standard deviation (SD). One-way analysis of variance (ANOVA) was employed for analyzing multi-group data, followed by pairwise comparison using the least significant difference (LSD) test. A significance level of $p < 0.05$ was considered statistically significant. Statistical analyses and graph generation were conducted using GraphPad Prism 5 software.

3. Results

3.1. Active compounds and potential targets of CHYS

Utilizing the TCMSP database, we retrieved a total of 624 active compounds from the six herbal medicines in CHYS, comprising 349

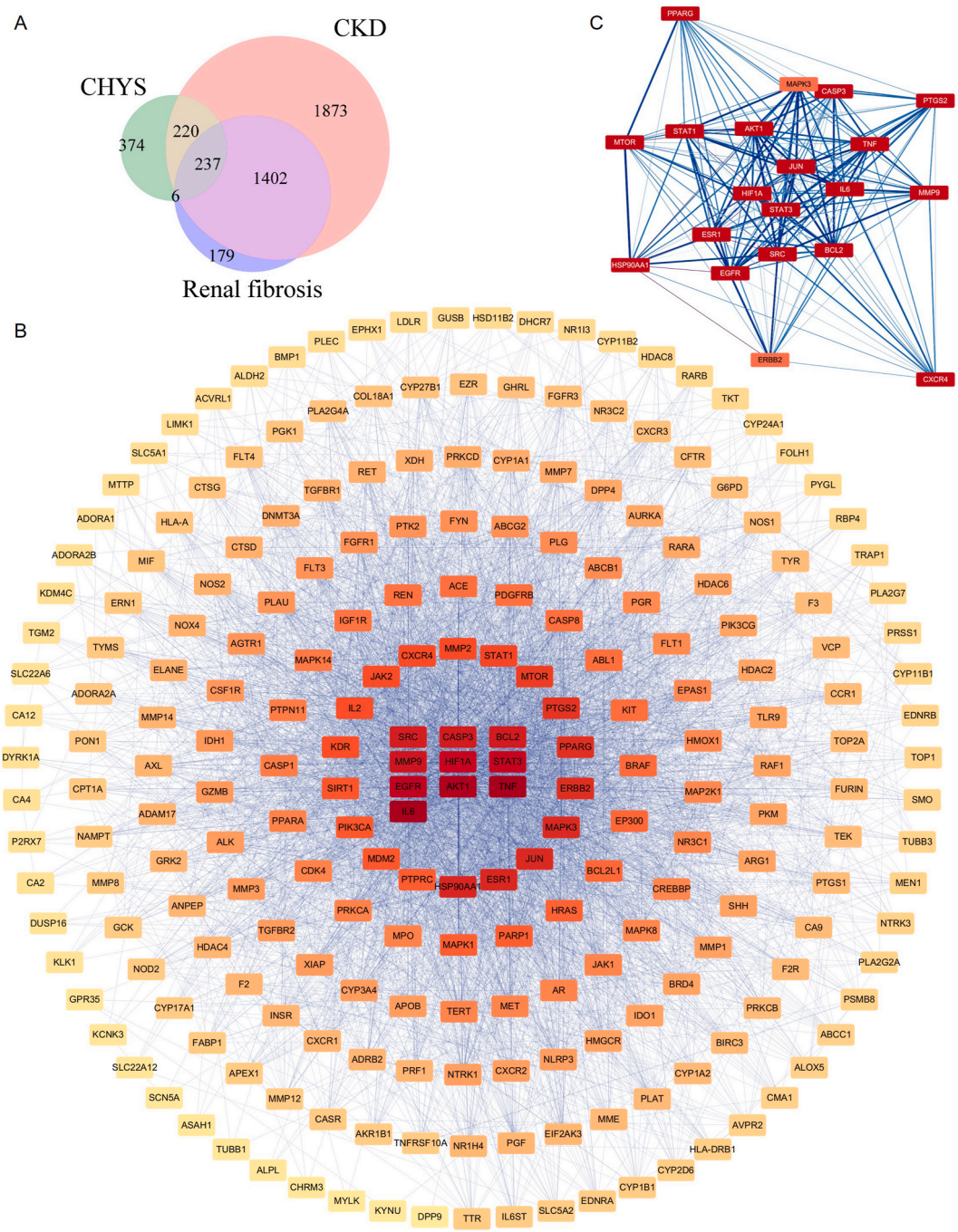

Fig. 2. PPI network analysis with drug-disease targets. (A) Venn diagram to show the intersection of targets among CHYS, CKD, and renal fibrosis. (B) PPI network comprising 237 drug-disease targets. Targets are represented by rectangles, with darker colors indicating higher degrees of centrality within the network. (C) Second round of PPI network analysis using the top 20-ranked targets identified in panel B.

components in Chaihu (CH), 87 in Huangqi (HQ), 125 in Danggui (DG), 23 in Shiwei (SW), 31 in Zhuling (ZL), and 9 in Chuanshanlong (CSL) (Supplementary Table 3). These compounds were then filtered to meet the criteria of oral bioavailability (OB) $\geq$ 30 % and druglikeness (DL) $\geq$ 0.18. Shuizhi (SZ), the sole animal-derived medicine, was not indexed in the TCMSP database. So, we gathered its 66 active compounds from published literature (Supplementary Table 3) [15–18], and subjected them to filtration based on gastrointestinal absorption and druglikeness criteria, as detailed in the methods. This process resulted in the identification of 96 active compounds (20 from HQ, 17 from CH, 11 from ZL, 6 from SW, 3 from CSL, 2 from DG, and 44 from SZ) (Supplementary Tables 4 and 5). Notably, several active compounds were found to be shared among multiple herbal medicines, such as kaempferol and quercetin in

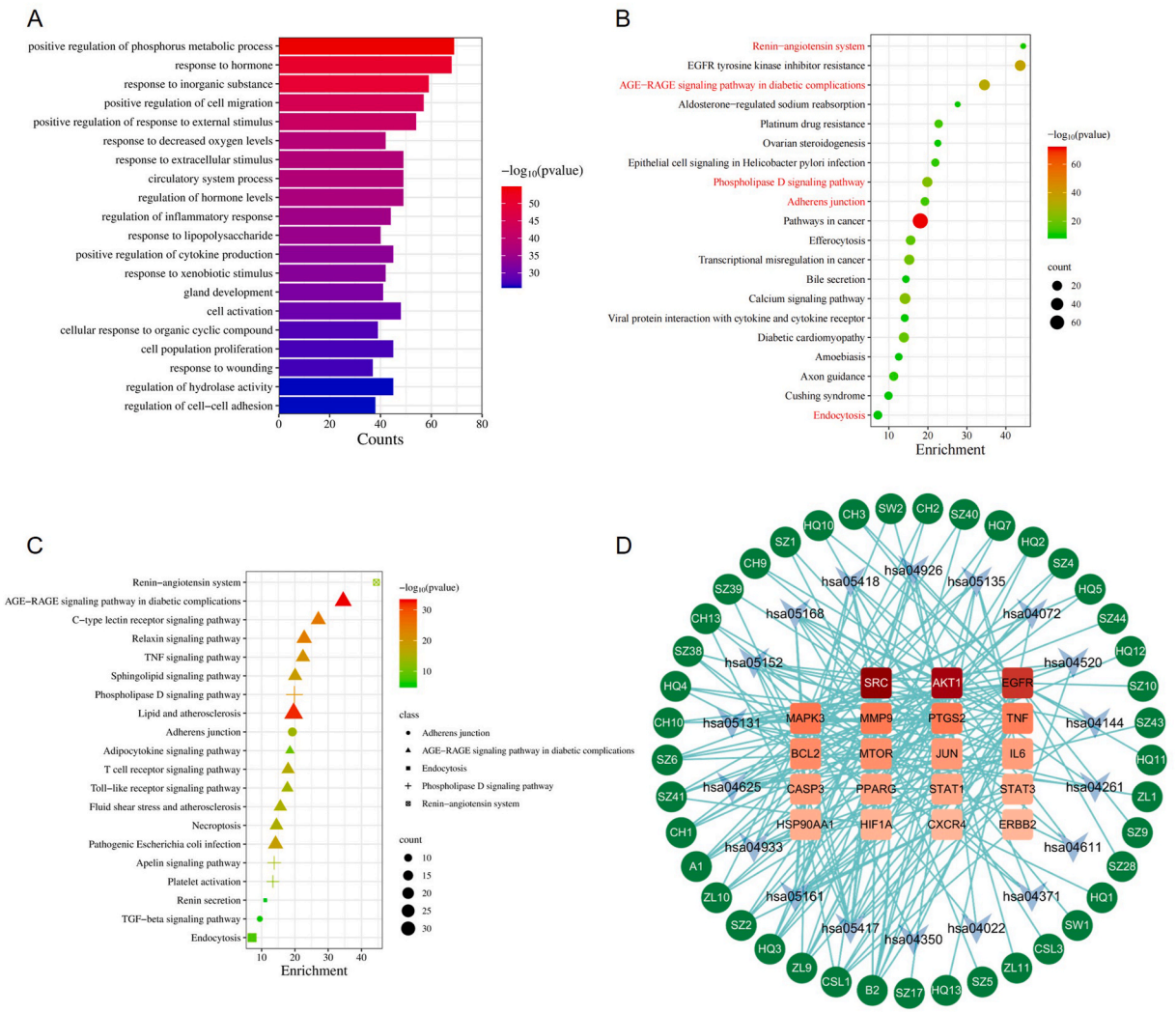

Fig. 3. Enrichment analysis and compound-target-pathway network. (A) Top 20 enriched biological processes (BP) identified through GO analysis using the 237 drug-disease targets. (B) Top 20 enriched pathways identified at the summary level in KEGG analysis with the 237 drug-disease targets. (C) Expansion of 20 enriched pathways derived from five higher-level renal fibrosis-related KEGG pathways. (D) Compound-target-pathway network. Circles stand for compounds, arrows for pathways, and rectangles for targets. The intensity of red color corresponds to the degree of centrality of the respective target.

HQ, CH, and SW, stigmasterol in both CH and DG, isorhamnetin in both CH and HQ, and beta-sitosterol in both DG and SW.

Subsequently, the protein targets of the 96 active compounds were predicted using the web-based SwissTargetPrediction platform. By considering a probability greater than 0 and removing duplicates, a total of 837 potential targets were identified (Supplementary Table 6). The network depicting reciprocal relationship between the active compounds and their corresponding targets in CHYS was visualized using Cytoscape software, as illustrated in Fig. 1B.

3.2. Discovery of common targets between CHYS and renal fibrosis in CKD

To identify common targets between CHYS and renal fibrosis in CKD, disease-related target genes were extracted from the GeneCards database using the keywords "chronic kidney disease" and "renal fibrosis," with a "relevance score" greater than 10. This yielded 3732 CKD-related targets and 1824 renal fibrosis-related targets (Supplementary Table 6). After intersection, 237 drug-disease targets were identified as shared by CHYS, CKD, and renal fibrosis (Fig. 2A and Supplementary Table 6).

3.3. PPI network analysis of the drug-disease targets

To identify key targets contributing to the treatment of renal fibrosis by CHYS, the protein-protein interaction (PPI) network was

Table 2
Top 10 compounds revealed by the compound-target-pathway analysis responsible for the anti-renal fibrosis effect of CHYS in CKD treatment.

ID	MolID	Compound	Degree	Betweenness Centrality	Closeness Centrality
B2	MOL000422	kaempferol	9	0.018	0.425
CSL1	MOL000133	7-Epitaxol	6	0.023	0.375
HQ3	MOL000239	Jaranol	5	0.018	0.425
SZ2	NA	cyclo(L-Pro-L-Phe)	5	0.010	0.371
ZL9	MOL000820	polyporusterone E	5	0.016	0.379
A1	MOL000354	isorhamnetin	4	0.007	0.386
CH1	MOL000490	petunidin	4	0.007	0.386
SZ41	NA	methyl 4-methyltetradecanoate	4	0.009	0.368
SZ6	NA	hirudinoidine A	4	0.016	0.403
ZL10	MOL000822	polyporusterone G	4	0.008	0.371

Table 3
Top 6-ranked targets responsible for the anti-renal fibrosis effect of CHYS revealed by the compound-target-pathway network.

Targets	Degree	Betweenness Centrality	Closeness Centrality
SRC	22	0.156	0.450
AKT1	21	0.113	0.440
EGFR	21	0.188	0.445
MAPK3	18	0.152	0.430
MMP9	17	0.091	0.430
PTGS2	17	0.090	0.425

constructed using the 237 drug-disease targets in the STRING platform, followed by visualization in Cytoscape software. The resultant PPI network encompassed 236 nodes and 4579 edges with an average node degree of 38.8 (Fig. 2B and Supplementary Table 7). Within the PPI network, a greater degree of centrality (color of the node) indicates a more important role it executes for a given target (node) [19]. The top 20-ranked targets with the highest degree of connectivity comprise IL6, TNF, AKT1, EGFR, STAT3, HIF1A, MMP9, BCL2, CASP3, SRC, HSP90AA1, ESR1, JUN, MAPK3, ERBB2, PPARG, PTGS2, MTOR, STAT1, and CXCR4. Subsequently, we performed a second round of PPI analysis with the top 20-ranked targets to elucidate their interactions more distinctly (Fig. 2C). This analysis revealed 22 target-target (protein-protein) interactions with a "combined score" exceeding 0.99 (Supplementary Table 7), suggesting robust associations among the 20 targets.

3.4. GO and KEGG analysis

Utilizing the 237 drug-disease targets, GO analysis unveiled 563 biological processes, which are classified into 20 distinct groups due to redundancy within enriched GO terms (Fig. 3A and Supplementary Table 8). Notably, among these groups, two biological processes, namely "response to wounding" [20] and "regulation of cell-cell adhesion" [21], emerged to be closely associated with renal fibrosis.

Following GO analysis, KEGG enrichment analysis was conducted employing the same 237 drug-disease targets. The top 20 enriched pathways, grouped at a higher level, are depicted in Fig. 3B, taking into consideration the redundancy of enriched terms (Supplementary Table 9). Of particular interest, five pathways demonstrated substantial involvement in renal fibrosis, including the "Renin-angiotensin system" [22], "AGE-RAGE signaling pathway" [23], "Phospholipase D signaling pathway" [24], "Adherens junction" [25], and "Endocytosis" [26]. Subsequently, a finer examination was undertaken at the item level within these five pathway groups, revealing 20 KEGG pathways directly implicated in renal fibrosis, among which the "Renin-angiotensin system" and "TGF-beta signaling pathway" were noteworthy.

3.5. Compound-target-pathway network analysis

To delve deeper into the potential mechanisms underlying CHYS's efficacy in treating renal fibrosis, we constructed the compound-target-pathway network using the 92 active compounds of CHYS, the top 20 targets delineated in Fig. 2C, and the 20 renal fibrosis-associated pathways elucidated in Fig. 3C. As shown in Fig. 3D, 41 out of the 92 compounds, 19 out of the 20 targets, and 18 out of the 20 pathways manifested reciprocal interconnections within the compound-target-pathway network. Notably, among these compounds, kaempferol (B2) emerged with the highest degree value of 9, accompanied by a centrality value of 0.43. It exhibited connections to targets AKT1, EGFR, MMP9, PTGS2, SRC, AKT1, EGFR, MMP9, and SRC (Table 2 and Fig. 3D). Among these targets, SRC, AKT1, and EGFR are top 3-ranked with a degree value surpassing 20 (Table 3). Notably, SRC and AKT1 were identified as core signaling regulators across most of the renal fibrosis-associated pathways (highlighted in Table 4). Moreover, previous studies have underscored the pivotal roles of SRC and AKT1 in CKD-associated renal fibrosis and SRC serves as an upstream activator of AKT1 [27–29]. Thus, the compound-target-pathway network analysis indicated that SRC and AKT1 are the potential targets responsible for CHYS's anti-renal fibrosis effects, warranting further downstream validation studies.

Table 4
The 20 renal fibrosis-related KEGG pathways enriched in the drug-disease targets.

ID	Description	Enrichment score	Count	%	Log10(P)	Genes in the Hits
hsa04614	Renin-angiotensin system	44.46	8.00	3.38	-11.26	AGTR1,ANPEP,CMA1,CTSG,ACE,KLK1,MME,REN,ADORA1,ADRB2,EDNRA
hsa04933	AGE-RAGE signaling pathway in diabetic complications	34.51	27.00	11.39	-33.47	AGTR1,AKT1,BCL2,CASP3,CDK4,MAPK14,F3,HRAS,IL6,JAK2,JUN,MMP2,PIK3CA,PRKCA,PRKCB,PRKCD,CASP8,CYP1A1,ERN1,HSP90AA1,LDLR,MMP1,MMP3,MMP9,PPARG,PTK2,SRC,TNFRSF10A, etc.
hsa04625	C-type lectin receptor signaling pathway	27.04	22.00	9.28	-24.74	AKT1,CASP1,CASP8,MAPK14,HRAS,IL2,IL6,JUN,MDM2,PIK3CA,PRKCD,MAPK1,MAPK3,MAPK8,MAPK10,PTGS2,PTPN11,RAF1,SRC,STAT1,TNF,NLRP3
hsa04926	Relaxin signaling pathway	22.79	23.00	9.70	-24.02	AKT1,MAPK14,EDNRB,EGFR,HRAS,JUN,MMP1,MMP2,MMP9,NOS1,NOS2,PIK3CA,PRKCA,MAPK1,MAPK3,MAPK8,MAPK10,MAP2K1,RAF1,SRC,TGFBR1,TGFBR2,VEGFA
hsa04668	TNF signaling pathway	22.42	20.00	8.44	-20.78	AKT1,BIRC3,XIAP,CASP3,CASP8,MAPK14,IL6,JUN,MMP3,MMP9,MMP14,PIK3CA,MAPK1,MAPK3,MAPK8,MAPK10,MAP2K1,PTGS2,TNF,NOD2
hsa04071	Sphingolipid signaling pathway	20.07	19.00	8.02	-18.81	ADORA1,AKT1,ASAH1,BCL2,MAPK14,CTSD,FYN,HRAS,ABCC1,PIK3CA,PRKCA,PRKCB,MAPK1,MAPK3,MAPK8,MAPK10,MAP2K1,RAF1,TNF
hsa04072	Phospholipase D signaling pathway	19.86	23.00	9.70	-22.58	AGTR1,AKT1,AVPR2,EGFR,F2,F2R,MTOR,FYN,HRAS,CXCR1,CXCR2,INSR,KIT,PDGFRB,PIK3CA,PIK3CG,PLA2G4A,PRKCA,MAPK1,MAPK3,MAP2K1,PTPN11,RAF1,MYLK,NOS1,NOS2,PLAT,TGFBR1,HDAC4,MAPK14,PTGS1,SRC,ADORA1,ADRB2,EDNRA,EDNRB,BCL2,SCN5A
hsa05417	Lipid and atherosclerosis	19.62	33.00	13.92	-32.14	AKT1,APOB,BCL2,BCL2L1,CASP1,CASP3,CASP8,MAPK14,CYP1A1,ERN1,HRAS,HSP90AA1,IL6,JAK2,JUN,LDLR,MMP1,MMP3,MMP9,PIK3CA,PPARG,PRKCA,MAPK1,MAPK3,MAPK8,MAPK10,PTK2,SRC,STAT3,TNF,TNFRSF10A,EIF2AK3,NLRP3
hsa04520	Adherens junction	19.24	14.00	5.91	-13.73	CREBBP,EGFR,EP300,ERBB2,FGFR1,FYN,IGF1R,INSR,MET,MAPK1,MAPK3,SRC,TGFBR1,TGFBR2,HDAC2,TNF
hsa04920	Adipocytokine signaling pathway	18.52	10.00	4.22	-9.79	AKT1,CPT1A,MTOR,JAK2,PPARA,MAPK8,MAPK10,PTPN11,STAT3,TNF
hsa04660	T cell receptor signaling pathway	17.96	17.00	7.17	-16.03	AKT1,CDK4,MAPK14,FYN,HRAS,IL2,JUN,PIK3CA,MAPK1,MAPK3,MAPK8,MAPK10,MAP2K1,PTPN11,PTPRC,RAF1,TNF
hsa04620	Toll-like receptor signaling pathway	17.75	15.00	6.33	-14.13	AKT1,CASP8,MAPK14,IL6,JAK1,JUN,PIK3CA,MAPK1,MAPK3,MAPK8,MAPK10,MAP2K1,STAT1,TNF,TLR9
hsa05418	Fluid shear stress and atherosclerosis	15.63	17.00	7.17	-14.99	AKT1,BCL2,MAPK14,HMOX1,HSP90AA1,JUN,KDR,MMP2,MMP9,PIK3CA,PLAT,MAPK8,MAPK10,PTK2,SRC,TNF,VEGFA
hsa04217	Necroptosis	14.47	18.00	7.59	-15.24	PARP1,BIRC3,XIAP,BCL2,CASP1,CASP8,HSP90AA1,JAK1,JAK2,PLA2G4A,MAPK8,MAPK10,PYGL,STAT1,STAT3,TNF,TNFRSF10A,NLRP3
hsa05130	Pathogenic Escherichia coli infection	14.20	22.00	9.28	-18.35	ABL1,CASP1,CASP3,CASP8,MAPK14,F2,F2R,FYN,IL6,JUN,MAPK1,MAPK3,MAPK8,MAPK10,PTPN11,SRC,TNF,EZR,TNFRSF10A,TUBB3,TUBB1,NLRP3
hsa04371	Apelin signaling pathway	13.79	15.00	6.33	-12.48	AGTR1,AKT1,MTOR,HRAS,MYLK,NOS1,NOS2,PIK3CG,PLAT,MAPK1,MAPK3,MAP2K1,RAF1,TGFBR1,HDAC4
hsa04611	Platelet activation	13.40	13.00	5.49	-10.72	AKT1,MAPK14,F2,F2R,FYN,MYLK,PIK3CA,PIK3CG,PLA2G4A,MAPK1,MAPK3,PTGS1,SRC
hsa04924	Renin secretion	11.11	6.00	2.53	-4.77	ADORA1,ADRB2,AGTR1,ACE,EDNRA,REN
hsa04350	TGF-beta signaling pathway	9.47	8.00	3.38	-5.65	CREBBP,EP300,HDAC2,MAPK1,MAPK3,TGFBR1,TGFBR2,TNF
hsa04144	Endocytosis	7.16	14.00	5.91	-7.90	GRK2,EGFR,FGFR3,HLA-A,HRAS,IGF1R,CXCR1,CXCR2,LDLR,MDM2,SRC,TGFBR1,TGFBR2,CXCR4

Note: The core targets SRC and AKT1 were highlighted in yellow background.

3.6. Investigation of the effect of CHYS administration on the expression of core target genes in the UUO mouse model of CKD-associated renal fibrosis

To investigate the impact of CHYS on the expression of core target genes identified through network pharmacology, we conducted experiments in the UUO mouse model, a well-established model of CKD characterized by typical renal fibrosis. Post-surgery, UUO mice received daily oral administrations of CHYS at doses of 3.8 (CHYS-L) and 7.6 g/kg/day (CHYS–H), respectively, for a duration of 7 days. Histological examination using HE and PAS staining revealed widespread tubular epithelial dilation, necrosis, degeneration, and

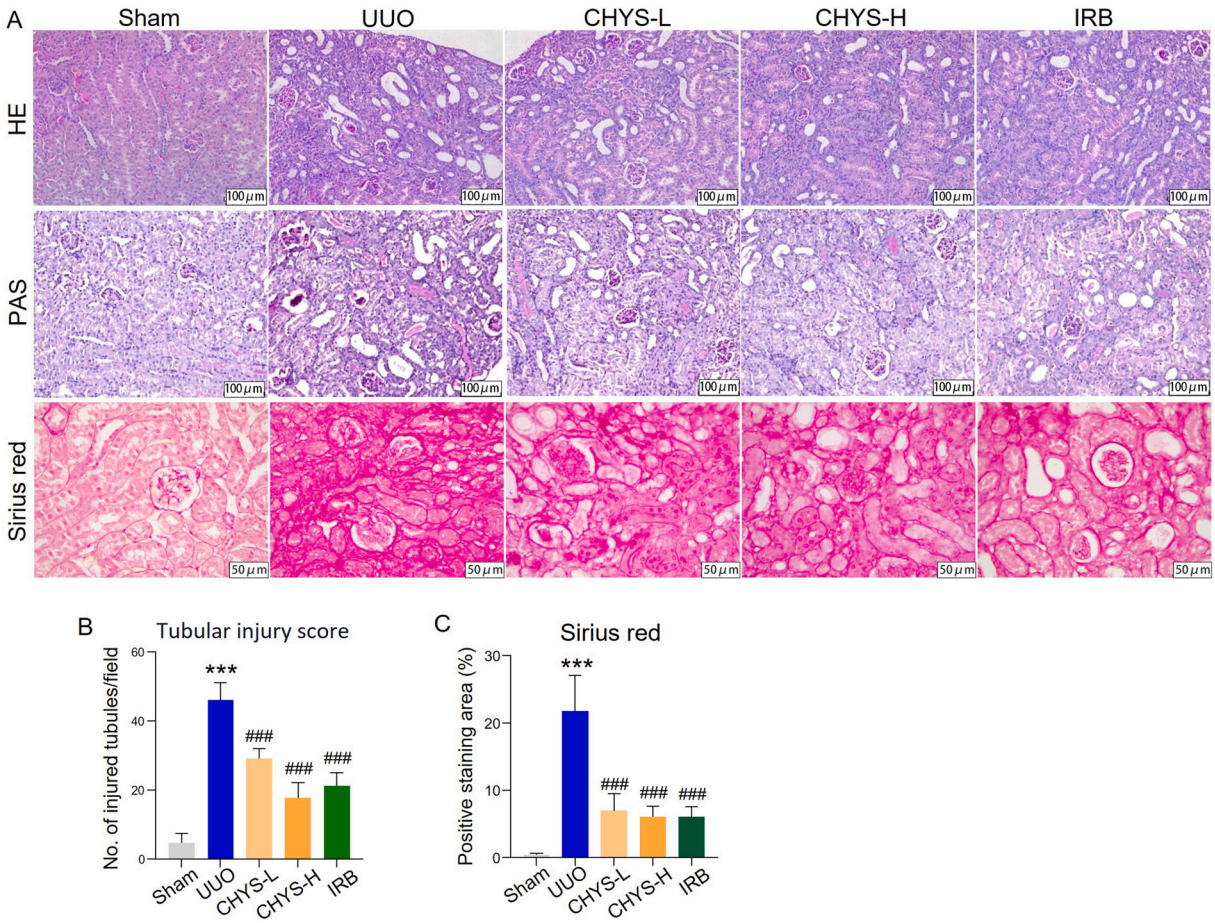

Fig. 4. CHYS treatment attenuates renal fibrosis in UUO mice. (A) Representative images of HE, PAS, and Sirius red staining of kidney sections, respectively. (B) Quantitation of tubular injury score based on PAS staining. (C) Quantitation of positive area of Sirius red staining. n = 6 animals for each group in B and C. $^{***}p < 0.001$ versus Sham. $^{###}p < 0.001$ versus UUO. IRB denotes irbesartan.

interstitial expansion, leading to an increased tubular injury score in UUO kidneys (Fig. 4A and B). Sirius red staining also demonstrated massive interstitial collagen fiber distribution in UUO kidney sections (Fig. 4A and C). However, treatment with CHYS at both dosage levels notably ameliorated these structural abnormalities and reduced collagen fiber deposition. Further analysis via RT-PCR, immunohistochemistry, and Western blot revealed elevated mRNA and protein expression of fibrosis markers, including fibronectin, α-smooth muscle actin (α-SMA), and Col1a1 (or collagen I), in UUO kidneys. CHYS treatment significantly suppressed the expression of these fibrosis markers (Fig. 5). Consistent with previous findings [30], the positive control drug irbesartan (IRB) also exhibited renoprotective effects against UUO-induced fibrosis (Figs. 4 and 5).

We next investigated the expression of core target genes *Src* and *Akt1* in CHYS-treated UUO mice. RT-PCR analysis demonstrated elevated mRNA levels of *Src* and *Akt1* in UUO kidneys. Notably, CHYS treatment significantly downregulated *Src* mRNA expression at both dosage levels, while *Akt1* mRNA levels were unaffected in CHYS-treated UUO kidneys (Fig. 6A and B). Western blot assay confirmed increased expression of Src, Akt1, and their phosphorylated forms (p-Src and p-Akt1) in UUO kidneys. CHYS treatment led to reductions in both total Src protein levels and p-Src. While total Akt1 protein levels remained relatively unchanged following CHYS treatment, Akt1 phosphorylation was significantly suppressed in UUO kidneys treated with both dosages of CHYS (Fig. 6C–G). Consistent with the Western blot data, immunohistochemistry also showed increased staining of Src, p-Src, Akt1, and p-Akt1 in UUO kidney sections compared to sham-operated kidney sections. CHYS treatment reduced the staining of Src, p-Src, and p-Akt1 at both dosages, though the staining of Akt1 was not significantly affected. As Src is upstream of Akt1 and both contribute to renal fibrosis [27,31], these data validate the findings of network pharmacology, demonstrating that CHYS inhibits profibrotic Src/Akt1 signaling axis to combat renal fibrosis.

4. Discussion

The Chinese medical formula CHYS has presented validated clinical efficacy in CKD treatment [7,32]. Animal experiments have further substantiated CHYS's therapeutic potential in attenuating renal fibrosis in mice afflicted with UUO and DN [9–11]. In this

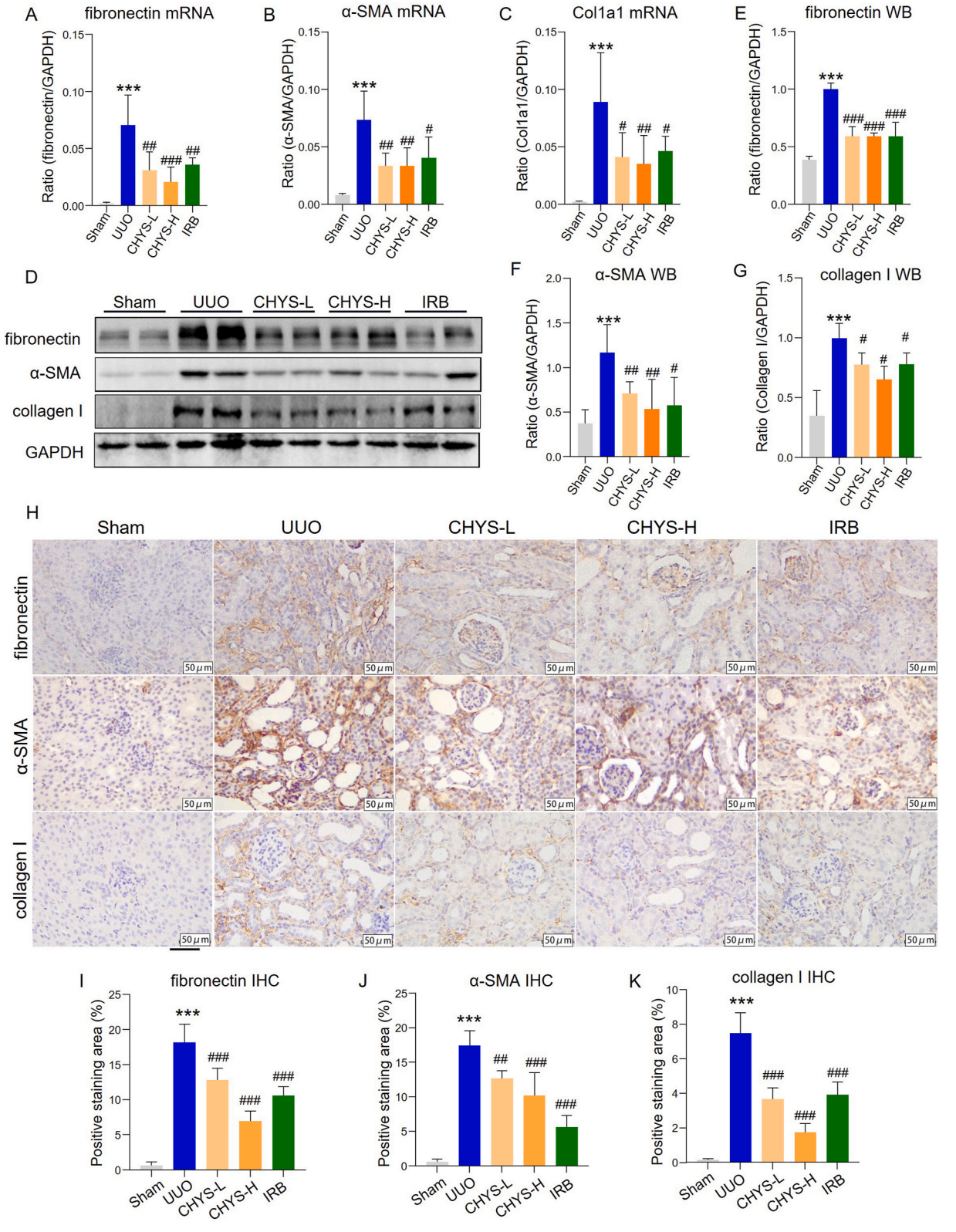

(caption on next page)

Fig. 5. CHYS treatment suppresses the expression of fibrotic marker genes in UUO mice. (A–C) RT-PCR to quantitate the mRNA levels of *fibronectin*, *α-SMA*, and *Col1a1*. n = 6 animals for each group. (D) Western blot to analyze the protein expression of fibronectin, α-SMA, and collagen I. E to G are quantitation of corresponding protein bands in D. n = 4 animals for each group. (H) Representative images of IHC staining of fibronectin, α-SMA, and collagen I in kidney sections. I to K are quantitation of positive staining area for each fibrosis marker proteins in H, respectively. n = 6 animals for each group. $^{***}p < 0.001$ versus Sham. $^{\#}p < 0.05$, $^{\#\#}p < 0.01$, and $^{\#\#\#}p < 0.001$ versus UUO. IRB stands for irbesartan.

study, network pharmacology was employed to dissect the potential mechanisms underlying CHYS's anti-renal fibrotic efficacy. From seven herbal/animal medicines, we identified 96 active compounds and 837 disease-related target genes, of which 237 were associated with CKD and renal fibrosis (Fig. 2). Enrichment analysis of these targets revealed modulation of multiple fibrosis-related biological processes and signaling pathways, including "response to wounding" and "regulation of cell-cell adhesion" in GO analysis, and "adherens junction" and "TGF-beta signaling pathway" in KEGG analysis.

Detailed analysis of the compound-target-pathway network unveiled SRC and AKT1 as pivotal targets. Both proteins, classified as protein kinases, play crucial roles in various CKD-related signaling pathways (Table 4). Experimental evidence suggests a pathogenic role for SRC and AKT1 in renal fibrosis. SRC, a target gene of TGF-β/Smad3 signaling, mediates TGF-β1-induced macrophage to myofibroblast transition (MMT) and subsequent collagen production. Inhibition of SRC mitigates MMT-driven renal fibrosis in UUO mice [28]. Similarly, it is recently reported that Akt1 is activated during AKI (acute kidney injury)-to-CKD transition. Deletion of Akt1 attenuates renal fibrosis, tubular epithelial-to-mesenchymal transition (EMT), tubular apoptosis in mice undergoing AKI-to-CKD transition [29]. More importantly, it is reported that Src is positioned upstream of Akt1 and can activate Akt1 signaling in glomerular mesangial cells and cancer cells [27,31].

Validation experiments in the UUO mouse model demonstrated that CHYS treatment attenuated structural injury and collagen deposition in the kidneys, accompanied by reduced expression of fibrotic genes fibronectin, α-SMA and collagen I (Col1a1) (Figs. 5 and 6), which is consistent with previous findings [32]. Notably, CHYS treatment downregulated mouse Src mRNA and protein levels, leading to decreased Src phosphorylation. Conversely, while CHYS did not notably affect Akt1 expression, it significantly suppressed Akt1 phosphorylation in UUO kidneys (Fig. 5). Therefore, these data validate the findings from network pharmacology analysis. Considering the important roles of Src and Akt1 in renal fibrosis of CKD and the evidence that Src can mediate the activation of Akt1, findings in this study suggest that CHYS may exerts its anti-renal fibrosis efficacy by suppressing the Src/Akt1 signaling.

Furthermore, the compound-target-pathway network analysis highlighted kaempferol as the top 1-ranked compound with the highest degree of centrality (B2 in Fig. 3D). Kaempferol is a flavonol present in Hunagqi, Chaihu, and Shiwei (Supplementary Table 3). Moreover, Src and Akt1 are both the predicted targets of kaempferol (Supplementary Table 6). Kaempferol demonstrates multiple activities [33]. It is reported that kaempferol attenuates renal fibrosis in chronic hypertension-induced CKD and suppresses TGF-β1-induced EMT and migration in human proximal tubular HK2 cells [34]. Furthermore, kaempferol can also reduce renal fibrosis in UUO rats with suppressed TGF-β1-triggered EMT in rat proximal tubular NRK-52E cells [35]. These findings underscore kaempferol as a key active compound contributing to CHYS's anti-renal fibrosis efficacy.

5. Conclusions

In summary, our study provides comprehensive insights into the molecular mechanisms underlying CHYS's therapeutic effects in combating renal fibrosis. The findings indicate that the suppression of Src/Akt1 signaling, along with the involvement of kaempferol, constitutes critical mechanisms of action that warrant further investigation.

Ethics statement

The animal experiments complied with corresponding regulations issued and were approved by the Animal Ethics Committee of Southwest Medical University (Ref. No. 20221205-031).

Funding

This work was supported by the National Natural Science Foundation of China (82174296), Sichuan Science and Technology Program (2022YFS0621), Luzhou-Southwest Medical University Science and Technology Strategic Cooperation Project (2021LZXNYD-P04), and Project of Southwest Medical University Affiliated Traditional Medicine Hospital (2022-CXTD-03).

Data availability Statement

The datasets (Supplementary Tables) for this study can be found in the Figshare database (https://doi.org/10.6084/m9.figshare.25464631).

CRediT authorship contribution statement

Jie Miao: Investigation, Formal analysis, Data curation. **Cong Wei:** Investigation. **Hong-Lian Wang:** Writing – original draft,

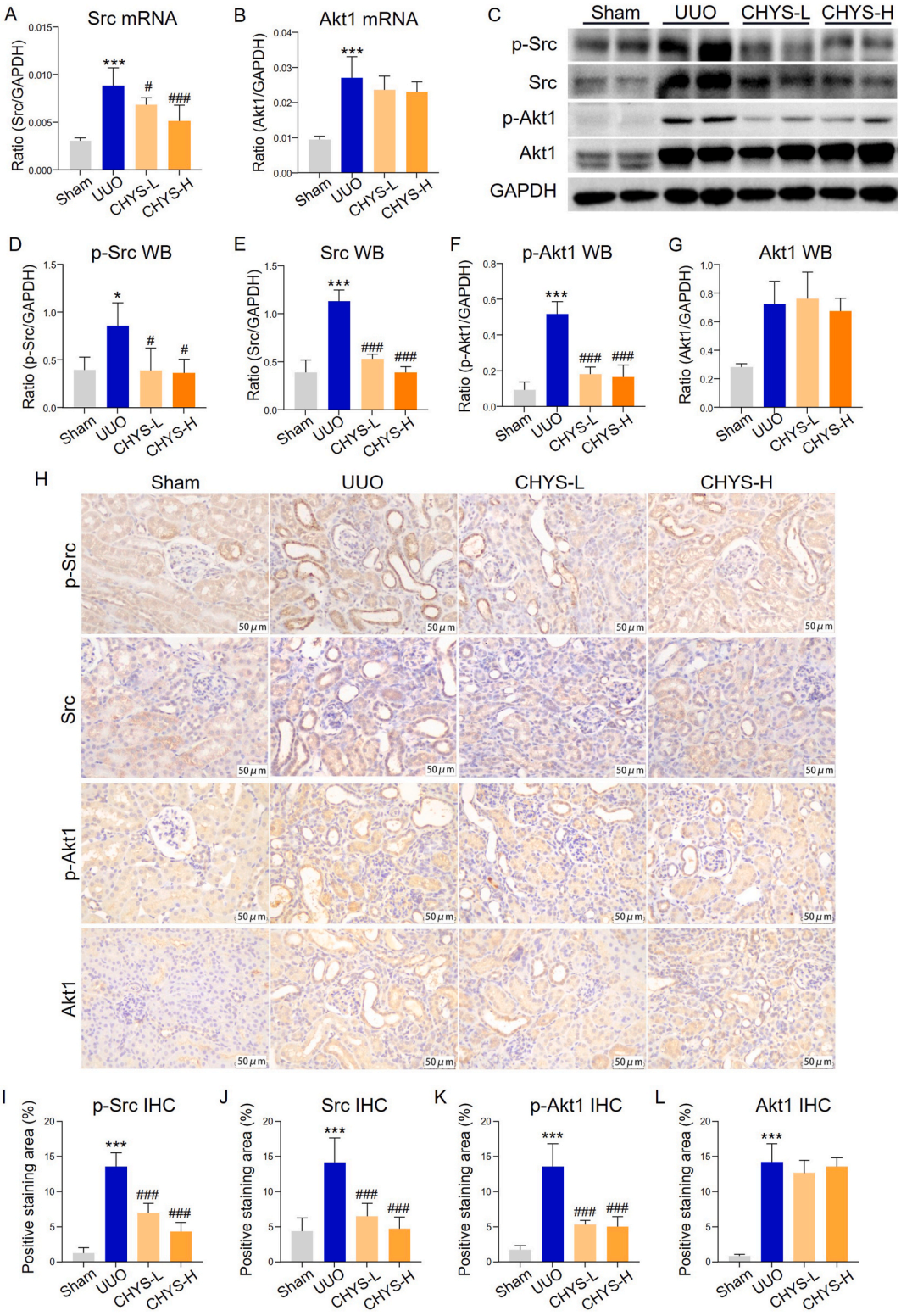

Fig. 6. CHYS treatment suppresses Src and Akt1 in UUO kidneys. (A and B) RT-PCR to detect the mRNA expression of *Src* and *Akt1* in kidney tissues. n = 6 animals in each group. (C) Western blot to detect the protein expression of p-Src, Src, p-Akt1, and Akt1 in kidney tissues. (D–G) Quantitation of corresponding proteins in C. n = 6 animals in each group. (H) Representative images of immunohistochemistry of Src, p-Src, Akt, and p-Akt in kidney tissues. (I–L) Quantitation of positive staining area in H. n = 6 animals in each group. $^{*}p < 0.05$ and $^{***}p < 0.001$ versus Sham. $^{\#}p < 0.05$ and $^{\#\#\#}p < 0.001$ versus UUO.

Validation. **Yu-Qing Li:** Data curation. **Xin-Ming Yu:** Methodology. **Xiu Yang:** Methodology. **Hong-Wei Su:** Methodology, Funding acquisition. **Ping Li:** Supervision, Funding acquisition. **Li Wang:** Supervision, Funding acquisition, Conceptualization.

Declaration of competing interest

The authors declare the following financial interests/personal relationships which may be considered as potential competing interests: Ping Li reports financial support was provided by National Natural Science Foundation of China. Hong-Wei Su reports financial support was provided by Sichuan Province Science and Technology Support Program. Li Wang reports financial support was provided by Luzhou-Southwest Medical University Science and Technology Strategic Cooperation Project. Li Wang reports financial support was provided by The Affiliated Hospital of Traditional Chinese Medicine of Southwest Medical University. If there are other authors, they declare that they have no known competing financial interests or personal relationships that could have appeared to influence the work reported in this paper.

Appendix A. Supplementary data

Supplementary data to this article can be found online at https://doi.org/10.1016/j.heliyon.2024.e35728.

References

[1] T.K. Chen, D.H. Knicely, M.E. Grams, Chronic kidney disease diagnosis and management: a review, JAMA 322 (13) (2019) 1294–1304, https://doi.org/10.1001/jama.2019.14745.

[2] L. Wang, et al., TGF-beta as a master regulator of diabetic nephropathy, Int. J. Mol. Sci. 22 (15) (2021), https://doi.org/10.3390/ijms22157881.

[3] U. Rende, et al., Diagnostic and prognostic biomarkers for tubulointerstitial fibrosis, J. Physiol. 601 (14) (2023) 2801–2826, https://doi.org/10.1113/JP284289.

[4] Y. Wang, et al., Traditional Chinese medicine in the treatment of chronic kidney diseases: theories, applications, and mechanisms, Front. Pharmacol. 13 (2022) 917975, https://doi.org/10.3389/fphar.2022.917975.

[5] K.C. Huang, et al., Chinese herbal medicine improves the long-term survival rate of patients with chronic kidney disease in taiwan: a nationwide retrospective population-based cohort study, Front. Pharmacol. 9 (2018) 1117, https://doi.org/10.3389/fphar.2018.01117.

[6] P. Li, et al., Efficacy and safety of tangshen formula on patients with type 2 diabetic kidney disease: a multicenter double-blinded randomized placebo-controlled trial, PLoS One 10 (5) (2015) e0126027, https://doi.org/10.1371/journal.pone.0126027.

[7] T. Zhao, et al., Metabolomic and lipidomic study of the protective effect of Chaihuang-Yishen formula on rats with diabetic nephropathy, J. Ethnopharmacol. 166 (2015) 31–41, https://doi.org/10.1016/j.jep.2015.02.019.

[8] P. Li, et al., Chinese herbal formula Qilong-Lishui granule improves puromycin aminonucleoside-induced renal injury through regulation of bone morphogenetic proteins, Nephrology 12 (5) (2007) 466–473, https://doi.org/10.1111/j.1440-1797.2007.00828.x.

[9] H. Zhang, et al., Attenuation of diabetic nephropathy by Chaihuang-Yishen granule through anti-inflammatory mechanism in streptozotocin-induced rat model of diabetics, J. Ethnopharmacol. 151 (1) (2014) 556–564, https://doi.org/10.1016/j.jep.2013.11.020.

[10] T.T. Zhao, et al., Chaihuang-Yishen granule inhibits diabetic kidney disease in rats through blocking TGF-beta/Smad3 signaling, PLoS One 9 (3) (2014) e90807, https://doi.org/10.1371/journal.pone.0090807.

[11] L. Jia, et al., Improvment effect of Chaihuang Yisheng formaula on chronic nephropathy rat model [Chinese], Tradit. Chin. Drug Res. Clin. Pharmacol. 16 (6) (2005) 408–412, https://doi.org/10.19378/j.issn.1003-9783.2005.06.006.

[12] Z. Peng, et al., The Smad3-dependent microRNA let-7i-5p promoted renal fibrosis in mice with unilateral ureteral obstruction, Front. Physiol. 13 (2022) 937878, https://doi.org/10.3389/fphys.2022.937878.

[13] J. Jia, et al., Hederagenin ameliorates renal fibrosis in chronic kidney disease through blocking ISG15 regulated JAK/STAT signaling, Int. Immunopharm. 118 (2023) 110122, https://doi.org/10.1016/j.intimp.2023.110122.

[14] R.Z. Tan, et al., Quercetin protects against cisplatin-induced acute kidney injury by inhibiting Mincle/Syk/NF-kappaB signaling maintained macrophage inflammation, Phytother Res. 34 (1) (2020) 139–152, https://doi.org/10.1002/ptr.6507.

[15] J. He, et al., Mechanism of drug pair Astragali Radix-Hirudo against pulmonary fibrosis based on network pharmacology [Chinese], Mod Chin Med 24 (1) (2022) 59–69, https://doi.org/10.13313/j.issn.1673-4890.20201223007.

[16] L. Ouyang, et al., Mechanisms of Hirudo in promoting blood circulation and removing stasis based on network pharmacology [Chinese], China J. Chin. Mater. Med. 43 (9) (2018) 1901–1906, https://doi.org/10.19540/j.cnki.cjcmm.2018.0065.

[17] Q. Jiang, et al., Research progress on processing history evolution, chemical constituents, and pharmacological effects of Hirudo, China J. Chin. Mater. Med. 47 (21) (2022) 5806–5816, https://doi.org/10.19540/j.cnki.cjcmm.20220411.201.

[18] X. Guo, D. Hou, Y. Liu, Mechanism of Leech preventing osteonecrosis of femoral head based on network pharmacology [Chinese], Chin Arch Tradit Chin Med 39 (1) (2021) 235–240, https://doi.org/10.13193/j.issn.1673-7717.2021.01.057.

[19] A. Majeed, S. Mukhtar, Protein-protein interaction network exploration using Cytoscape, Methods Mol. Biol. 2690 (2023) 419–427, https://doi.org/10.1007/978-1-0716-3327-4_32.

[20] S.C. Huen, L.G. Cantley, Macrophages in renal injury and repair, Annu. Rev. Physiol. 79 (2017) 449–469, https://doi.org/10.1146/annurev-physiol-022516-034219.

[21] Y. Liu, Epithelial to mesenchymal transition in renal fibrogenesis: pathologic significance, molecular mechanism, and therapeutic intervention, J. Am. Soc. Nephrol. 15 (1) (2004) 1–12, https://doi.org/10.1097/01.asn.0000106015.29070.e7.

[22] S.A. Mezzano, M. Ruiz-Ortega, J. Egido, Angiotensin II and renal fibrosis, Hypertension 38 (3 Pt 2) (2001) 635–638, https://doi.org/10.1161/hy09t1.094234.

[23] B. Martin-Carro, et al., Role of klotho and AGE/RAGE-Wnt/beta-Catenin signalling pathway on the development of cardiac and renal fibrosis in diabetes, Int. J. Mol. Sci. 24 (6) (2023), https://doi.org/10.3390/ijms24065241.

[24] P. Trivedi, et al., Targeting phospholipase D4 attenuates kidney fibrosis, J. Am. Soc. Nephrol. 28 (12) (2017) 3579–3589, https://doi.org/10.1681/ASN.2016111222.

[25] I. Yamaguchi, et al., Vascular endothelial cadherin modulates renal interstitial fibrosis, Nephron Exp. Nephrol. 120 (1) (2012) e20–e31, https://doi.org/10.1159/000332026.

[26] M. Chen, X. Gu, Emerging roles of proximal tubular endocytosis in renal fibrosis, Front. Cell Dev. Biol. 11 (2023) 1235716, https://doi.org/10.3389/fcell.2023.1235716.

[27] T.C. Beadnell, et al., Src-mediated regulation of the PI3K pathway in advanced papillary and anaplastic thyroid cancer, Oncogenesis 7 (2) (2018) 23, https://doi.org/10.1038/s41389-017-0015-5.

[28] P.M. Tang, et al., The proto-oncogene tyrosine protein kinase Src is essential for macrophage-myofibroblast transition during renal scarring, Kidney Int. 93 (1) (2018) 173–187, https://doi.org/10.1016/j.kint.2017.07.026.
[29] I.Y. Kim, et al., Akt1 is involved in renal fibrosis and tubular apoptosis in a murine model of acute kidney injury-to-chronic kidney disease transition, Exp. Cell Res. 424 (2) (2023) 113509, https://doi.org/10.1016/j.yexcr.2023.113509.
[30] J. Li, et al., Tectorigenin protects against unilateral ureteral obstruction by inhibiting Smad3-mediated ferroptosis and fibrosis, Phytother Res. 36 (1) (2022) 475–487, https://doi.org/10.1002/ptr.7353.
[31] K. Block, et al., Nox4 NAD(P)H oxidase mediates Src-dependent tyrosine phosphorylation of PDK-1 in response to angiotensin II: role in mesangial cell hypertrophy and fibronectin expression, J. Biol. Chem. 283 (35) (2008) 24061–24076, https://doi.org/10.1074/jbc.M803964200.
[32] R. Tan, et al., Chaihuang Yishen granules improves renal fibrosis in mice with chronic kidney disease by inhibiting macrophagic mincle [Chinese], Tradit. Chin. Drug Res. Clin. Pharmacol. 34 (12) (2023) 1658–1667, https://doi.org/10.19378/j.issn.1003-9783.2023.12.002.
[33] S.P. Bangar, et al., Kaempferol: a flavonoid with wider biological activities and its applications, Crit. Rev. Food Sci. Nutr. 63 (28) (2023) 9580–9604, https://doi.org/10.1080/10408398.2022.2067121.
[34] Y. Guan, et al., Kaempferol inhibits renal fibrosis by suppression of the sonic hedgehog signaling pathway, Phytomedicine 108 (2023) 154246, https://doi.org/10.1016/j.phymed.2022.154246.
[35] X. Ji, et al., Kaempferol protects renal fibrosis through activating the BMP-7-smad1/5 signaling pathway, Biol. Pharm. Bull. 43 (3) (2020) 533–539, https://doi.org/10.1248/bpb.b19-01010.